3D Magneto-Optical Trap of Yttrium Monoxide

Alejandra L. Collopy,[1] Shiqian Ding,[1] Yewei Wu,[1] Ian A. Finneran,[1] Loïc Anderegg,[2] Benjamin L. Augenbraun,[2] John M. Doyle,[2] and Jun Ye[1]

[1]*JILA, National Institute of Standards and Technology and Department of Physics, University of Colorado, Boulder, Colorado 80309, USA*

[2]*Department of Physics and Center for Ultracold Atoms, Harvard University, Cambridge, Massachusetts 02138, USA*

(Received 2 August 2018; published 21 November 2018)

We report three-dimensional trapping of an oxide molecule (YO), using a radio-frequency magneto-optical trap (MOT). The total number of molecules trapped is $\sim 1.5 \times 10^4$, with a temperature of 4.1(5) mK. This diversifies the frontier of molecules that are laser coolable and paves the way for the second-stage narrow-line cooling in this molecule to the microkelvin regime. Futhermore, the new challenges of creating a 3D MOT of YO resolved here indicate that MOTs of more complex nonlinear molecules should be feasible as well.

DOI: 10.1103/PhysRevLett.121.213201

The last decade has seen considerable successes in the association of atomic quantum gases to produce ultracold molecules [1,2] and in sympathetic cooling of molecular ions with laser coolable atomic species [3] for further spectroscopic [4] or chemistry [5] studies. But, only very recently has laser cooling of neutral molecules directly from a beam to the millikelvin regime and below become viable. Other promising techniques for diverse molecule cooling include electro-optic cooling [6], which has been demonstrated for formaldehyde [7], and various deceleration techniques, such as Stark [8,9] or centrifugal deceleration [10]. Molecular laser cooling is expanding the number of species usable for cold molecule experiments where large dipole moments and strong intermolecular interactions exist, as well as enlarging the workspace for cold chemistry studies [11,12].

Laser cooling is only logistically feasible for a subset of molecules with sufficiently closed cycling transitions [13]. The first proposal for a molecular magneto-optical trap (MOT) identified five classes of diatomic molecules as being amenable to laser cooling and trapping [14], including halides, hydrides, oxides, carbides, and sulfides. However, only the fluorides SrF [15] and CaF [16–18] have thus far been loaded into 3D MOTs. Since the initial proposals for diatomic species, a large number of polyatomic pseudofluorides have also been identified as laser coolable [19,20] and this has been demonstrated with SrOH [21]. Additionally, even in the absence of laser cooling or trapping, quasi-closed cycling transitions that enable rapid photon cycling can be utilized for internal state preparation and efficient readout in precision measurement experiments such as searches for the electron electric dipole moment (EDM) [22–24], or parity violation (PV) [25]. Furthermore, extension of EDM and PV experiments to diatomic and polyatomic molecules that can be directly cooled in a MOT promises great advances in sensitivity, due to increased coherence times and suppression of systematic errors [22,26,27]. However, as laser cooling and trapping is extended to more diverse diatomic and polyatomic species, new complications in molecular structure will arise beyond those present in the alkaline-earth monofluorides studied to date. Our work with yttrium monoxide thus represents a crucial milestone in extending 3D MOTs beyond "simple" alkaline-earth diatomic molecules like SrF and CaF to more complex molecular species desirable for many applications in quantum science and technology [28,29].

Building on our earlier work of two-dimensional (2D) magneto-optical trapping [30] and longitudinal slowing of yttrium monoxide (YO) [31], in this Letter we report a 3D MOT of YO. This is the first realization of a MOT for an oxide molecule. Because of the presence of decay from an intermediate electronic state in the YO molecule, the particular choice of the repumping scheme becomes more important to maintain a quasi-closed cycling transition and a large optical scattering rate. The ground-to-intermediate state transition in YO is also amenable to further laser cooling, making this MOT instantiation a critical step towards the realization of narrow-line cooling in a molecule. As narrow-line cooling greatly expanded the physics available for alkaline-earth [32,33] and magnetic atoms [34], it too may yield rich fields of study for molecules.

The level structure of YO has been described in previous work [30,31,35], and so here we highlight only the most salient details. In order to achieve a nearly closed optical cycling transition in YO, we utilize one of the two schemes depicted in Fig. 1(a). Two repump lasers limit vibrational branching loss to the 10^{-6} level. By using the $N'' = 1 \rightarrow J' = 1/2$ transition, parity and angular momentum selection rules ensure rotational closure. However, because of leakage to the intermediate $A'^2\Delta_{3/2}$ state, molecules will

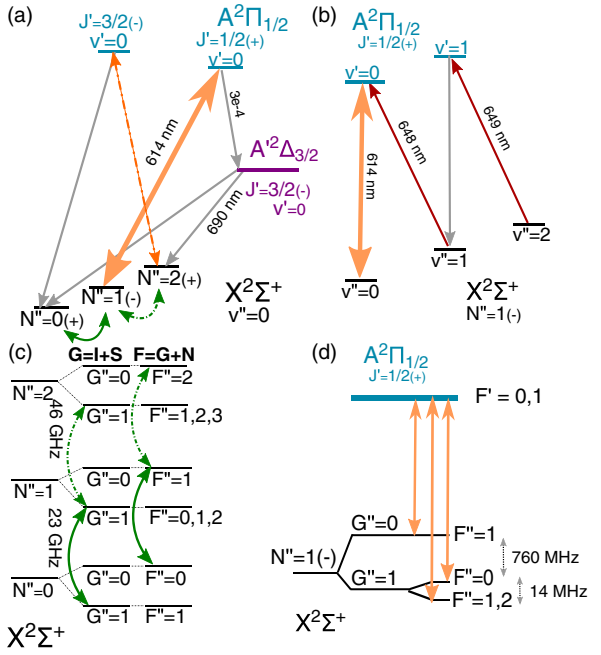

FIG. 1. Relevant level structure of the YO molecule. (a) The solid orange double-headed arrow indicates the main cooling transition, while green curved double-headed arrows depict microwave mixing. Gray arrows are decay channels. Dashed-dotted lines indicate various options we have for repumping states. (b) Red arrows indicate vibrational repump lasers which are used to limit unrecovered vibrational branching to the 10^{-6} level. (c) Microwaves couple molecular states of the same quantum number G. (d) Laser components address each hyperfine manifold separately.

decay to $X^2\Sigma(N''=0,2)$ after ~3000 photon-scattering events [31]. Although the transition from the $A'^2\Delta_{3/2}$ state to the $X^2\Sigma$ state is nominally forbidden, we find it does occur due to mixing of the $A'^2\Delta_{3/2}$ state with the nearby $A^2\Pi_{3/2}$ state, giving the $A'^2\Delta_{3/2}$ state a lifetime of ~1 μs [35]. We note that the transition wavelength to directly repump the $A'^2\Delta_{3/2}$ state to the $A^2\Pi_{1/2}(J=3/2)$ state is 5.6 μm and would be experimentally difficult to implement and frequency stabilize. To repump from $X^2\Sigma(N''=0)$, we apply microwaves at 23 GHz to remix the $X^2\Sigma(N''=0,1)$ levels. The microwaves couple states of same quantum number $\mathbf{G}=\mathbf{I}+\mathbf{S}$, and are modulated to cover the necessary hyperfine manifolds within $G=1$. To recycle the population in $X^2\Sigma(N''=2)$, we either use an optical repump to the $A^2\Pi_{1/2}(J'=3/2)$ level or use microwaves to directly remix the $X^2\Sigma(N''=1,2)$ levels, split by 46 GHz. Because of the number of states involved in the cycling transition, the optical repumper increases the scattering rate as opposed to microwave mixing by decoupling the $X^2\Sigma(N''=2)$ level from the main cycling transition. The change realized in this manner increases the maximum possible scattering rate from $\Gamma/13$ to $\Gamma/8$, a gain of a factor of 1.6, where $\Gamma=2\pi\times 5$ MHz is the natural linewidth of the $A^2\Pi_{1/2}$ state. In practice, with optical repumping of the $X^2\Sigma(N''=2)$ level, we realize a scattering rate of $\sim 10^6\ \mathrm{s}^{-1}$, which is measured by removing each vibrational repump and observing the rate of decay into a dark state in comparison with known Franck-Condon branching ratios, akin to the method used in Ref. [31].

Although the $X^2\Sigma(N''=1)\rightarrow A^2\Pi_{1/2}(J'=1/2)$ transition prevents rotational branching, it requires that we excite from a greater F'' to a smaller F'. This is often referred to as a type II cooling transition, as opposed to the type I transition more typically seen in atomic laser cooling experiments. In order to prevent decays into a dark m_F polarization state during slowing or trapping, it is necessary to utilize a remixing method. We modulate the polarization of our laser light between orthogonal linear (circular) polarization while slowing (trapping) at a rate of about 5 MHz. This rate was chosen because in our 1D cooling experiments the transverse laser-cooled temperature achieved continued to decrease up to that switching rate [30]. The polarization switching also necessitates care for the choice of magnetic fields during trapping, so as not to spend any time in an antitrapping configuration. As implemented previously for YO in one and two dimensions [30], we continue to use a radio frequency (rf) MOT in this 3D implementation. The polarization switching of the MOT beams is implemented with a Pockels cell to change between σ^+ and σ^- polarization synchronously with the magnetic field oscillation. While dc MOTs have been made for molecules, the effectiveness of this method relies on the small but nonzero magnetic g factor in the excited $A^2\Pi_{1/2}$ state [36] or a bichromatic scheme [16,37]. Comparisons between rf and dc MOTs for molecules have shown that the rf version provides a better performance [18,38].

The apparatus used to produce, decelerate, and trap the molecules is depicted in Fig. 2(a). In contrast to previous work on slowing of YO [31], we utilize a single stage cryogenic buffer gas cell as opposed to a two-stage cell. The single stage cell has larger peak molecule velocity (120 m/s instead of 70 m/s), but higher brightness. The molecules are produced via ablation of a Y_2O_3 ceramic target with a doubled (532 nm) Nd:YAG 7 mJ pulse. In order to improve the performance of the cell at low helium buffer gas flow rates, we find that coating the interior of the cell with a layer of Y_2O_3 nanopowder yields a larger flux of molecules for a given helium buffer gas flow rate. The nanopowder coating also brings the helium buffer gas flow rate that produces the maximal number of YO molecules from 8 to 2 sccm. The slowing laser beam is counter-propagating to the molecular beam. An in-vacuum shutter positioned 28 cm downstream from the buffer gas cell cuts off the continuous 0.5 sccm He flow after the YO molecule pulse has passed as well as preventing heating of the buffer gas cell due to the power in the slowing laser beam.

Our slowing scheme is similar to previous work [31], except that now, for simplicity, we no longer apply white

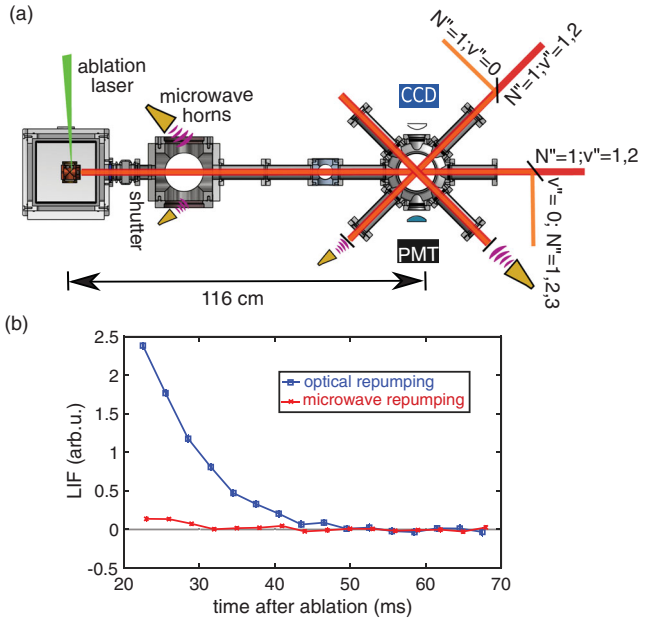

FIG. 2. (a) Top view of experimental apparatus. Molecules are produced at the left and travel to the right while interacting with a counterpropagating slowing beam. Slowed molecules are loaded into the MOT at the right, where they are imaged. Microwave horns are coupled into the chamber along the slowing region and in the MOT region. (b) Velocity sensitive detection of molecules at 5 m/s after the slowing sequence. The blue (square) line utilized optical repumping of $N'' = 2$ molecules, whereas the red (x) line used microwave repumping of these molecules. Error bars are within symbol size.

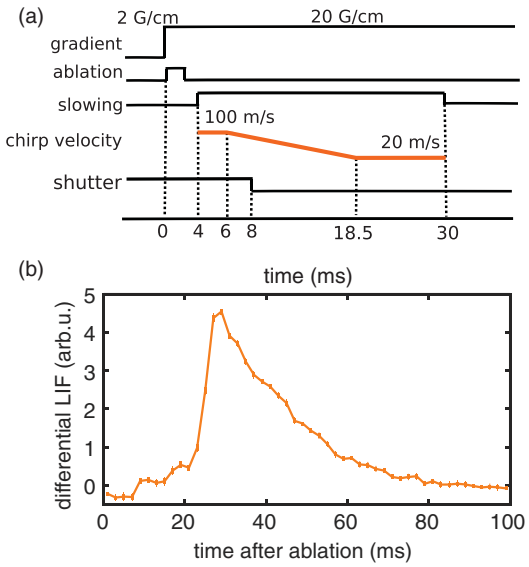

FIG. 3. (a) Timing sequence used for MOT production. MOT laser beams are on at all times. (b) Phase-subtracted LIF time trace of MOT loading and decay acquired from the PMT.

light modulation to the slowing beam. We maintain use of a frequency chirp, with variable duration and chirp range of 100 to 20 m/s, to continually address the molecules as they slow down. Microwaves are coupled into the chamber partway down the molecule slowing distance and into the MOT region with microwave horns. Molecules in the trap region are imaged with a charge-coupled device (CCD) camera for spatially resolved imaging, and with a photomultiplier tube (PMT) for time resolved information. We detect the laser induced fluorescence (LIF) of the molecules on the main cycling transition at 614 nm. We estimate our imaging photon collection efficiency to be about 0.3% and 0.1% for the CCD and PMT systems, respectively.

By frequency chirping the main cooling laser and repump lasers in the counterpropagating beam, we slow molecules from production speeds of approximately 120 m/s to trappable velocities of less than 5 m/s. We confirm the slowing by detecting the molecular LIF with a low-power Doppler sensitive probe beam at 45° with respect to the molecular beam propagation, as shown in Fig. 2(b). By changing from microwave to optical repumping of the $X^2\Sigma(N'' = 2)$ level (and a commensurate change in frequency chirp rate), we realize a gain in slowed molecule signal of a factor of 19. We estimate the total number of molecules slowed to 5 m/s using the optical repumping scheme of $X^2\Sigma(N'' = 2)$ to be about 1×10^5. When utilizing a higher scattering rate, we suffer less from the transverse divergence of the molecular beam due to less time required to reach the trapping region.

After slowing, molecules are loaded into the 3D MOT. The rf MOT coils in our experiment are an in-vacuum resonant circuit tunable from 3–5 MHz. By driving the circuit with 60 W (2 amps through each coil), we achieve a rms field gradient of 20 G/cm. A timing diagram used for loading molecules is shown in Fig. 3(a). We note that the slowing beam stays on during the loading of the MOT; its end point of 20 m/s is equivalent to 32 MHz detuning, and so serves to gently provide the last bit of slowing to the very slow molecules. Vibrational repumps are spatially overlapped with MOT beams, while $X^2\Sigma(N'' = 2, 3)$ are repumped along the slowing axis. In order to distinguish untrapped molecules still transiting the MOT region from the MOT itself, we examine a phase-subtracted differential signal of the correct phase minus 180° out of phase between the MOT coil drive and the polarization switching of the MOT beams.

The retroreflected MOT beams have a $1/e^2$ beam waist of 10 mm, and have 25 mW per beam of $v'' = 0$ light. Repump powers are typically 25 and 8 mW per MOT beam for $v'' = 1$ and 2, respectively, with 32 and 8 mW for $N'' = 2$ and 3 ($v'' = 0$), respectively. The LIF detected by the PMT using a 20 G/cm rms field gradient with 6 MHz red detuning of all $v'' = 0$ components is shown in Fig. 3(b). The peak number loaded into the trap is approximately 1.5×10^4 molecules (within a factor of 2), which we determine from our collection efficiency and peak photon scattering rate.

At normal MOT beam intensity, the $1/e$ lifetime of the MOT [as shown in Fig. 3(b)] is currently limited to ~20 ms

by an as-yet undetermined loss process. Optical repumping of the $X^2\Sigma(N''=3)$ level yields 30% more molecules in the MOT, but has no influence on the observed lifetime. We have also experimented with optical repumping of the $X^2\Sigma(v''=3)$ state via the $A^2\Pi_{1/2}(v'=2)$ state, which has not yet shown an effect in our experiment (consistent with the expected Franck-Condon factors for YO and the number of photons scattered). We originally suspected that the largest leak from our quasi-closed optical cycle was via the $A'^2\Delta_{3/2}$ state to the $X^2\Sigma(v''=1, N''=0,2)$ levels, but found that applying microwaves to remix those states did not increase the lifetime, implying the loss is due to a different mechanism. We do find that the lifetime of the MOT increases when the MOT beam intensity is lowered, at the expense of loaded molecule number.

To characterize the temperature of the MOT, as shown in Fig. 4, we load molecules into the MOT at 20 G/cm and 6 MHz red detuning, and then switch off the MOT beams to allow free expansion for a variable amount of time. By fitting the cloud to a Gaussian distribution and measuring the width as a function of free-flight time, we extract the radial and axial temperature of the MOT to be 4.1(5) and 3.8(5) mK, respectively. Based on the size and temperature of the molecular cloud, we apply the equipartition theorem to determine the radial and axial trap frequencies to be $f_{\mathrm{radial}} = 30$ and $f_{\mathrm{axial}} = 40$ Hz.

In conclusion, we demonstrate the three dimensional magneto-optical trapping of YO. To our knowledge, this represents the first MOT of a nonfluoride molecule, broadening the horizon of chemical diversity of cooled molecules to include an oxide which is of chemical [39] and astrophysical [40] relevance. It also represents the first MOT for a molecule with an electronic state intermediate to the main cycling transition states, which necessitates careful consideration of repump choice in order to rapidly cycle photons without losing molecules to dark states. Optical cycling in the presence of intermediate electronic states as well as decay to dark excited rotational levels both arise naturally when one is trying to create a MOT of nonlinear polyatomic molecules [20]. Our work with YO demonstrates that both of these issues can be efficiently resolved, opening the prospects of 3D MOTs for complex nonlinear molecules which have been proposed for a new generation of precision measurement [26] and quantum simulation experiments [41].

This realization of a MOT of YO is a necessary step for further narrow-line cooling on the 150 kHz transition from the $X^2\Sigma$ state to the $A'^2\Delta_{3/2}$ state at 690 nm as proposed in Ref. [35]. Narrow-line cooling on this transition will allow direct cooling to the microkelvin regime, allowing the molecules to be readily loaded into magnetic or optical dipole traps [17,42–44]. The transition has already been observed and characterized. Cooling on this transition will be experimentally more straightforward to implement than the initial trap due to a fewer number of photon scatterings needed for cooling and the ability to run in a type I MOT configuration at the expense of a reduced photon scattering rate. We also note that the finite lifetime of the first-stage broad linewidth MOT should be sufficient for loading to the second stage narrow-line MOT.

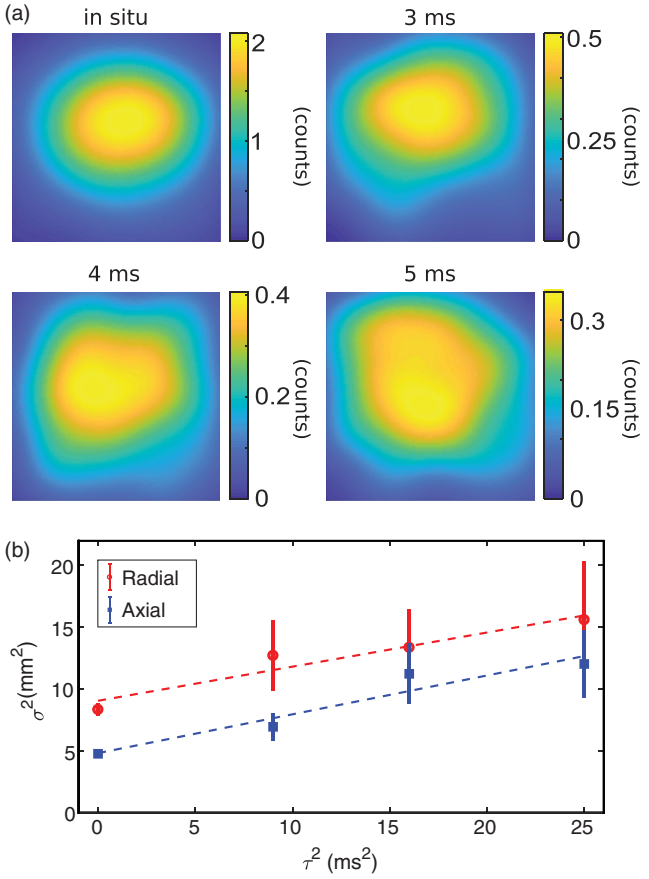

FIG. 4. MOT temperature characterization. The size of each image is 1 cm × 1 cm. (a) Phase-subtracted imaging of the MOT after some period of free expansion. The CCD exposure time is 2 ms for each image, and is the average of 180 experimental repetitions with a Gaussian filter of $\sigma = 1.5$ mm. (b) The measurement of the Gaussian width σ of the cloud in the axial and radial directions as a function of free flight time τ determines the temperature in these two directions. All fits are performed upon unsmoothed data.

We thank Ivan Kozyryev for feedback on the manuscript. We acknowledge funding support from ARO-MURI, the Gordon and Betty Moore Foundation, NIST, and the NSF Physics Frontier Centers JILA and CUA (Phys-1734006 and Phys-1734001). I. A. F. is supported by a National Research Council postdoctoral fellowship.

[1] K.-K. Ni, S. Ospelkaus, M. H. G. de Miranda, A. Pe'er, B. Neyenhuis, J. J. Zirbel, S. Kotochigova, P. S. Julienne, D. S. Jin, and J. Ye, Science **322**, 231 (2008).

[2] J. G. Danzl, M. J. Mark, E. Haller, M. Gustavsson, R. Hart, J. Aldegunde, J. M. Hutson, and H.-C. Nägerl, Nat. Phys. **6**, 265 (2010).
[3] E. R. Hudson, EPJ Tech. Instrum. **3**, 8 (2016).
[4] C.-w. Chou, C. Kurz, D. B. Hume, P. N. Plessow, D. R. Leibrandt, and D. Leibfried, Nature (London) **545**, 203 (2017).
[5] P. Puri, M. Mills, C. Schneider, I. Simbotin, J. A. Montgomery, R. Côté, A. G. Suits, and E. R. Hudson, Science **357**, 1370 (2017).
[6] M. Zeppenfeld, M. Motsch, P. W. H. Pinkse, and G. Rempe, Phys. Rev. A **80**, 041401 (2009).
[7] A. Prehn, M. Ibrügger, R. Glöckner, G. Rempe, and M. Zeppenfeld, Phys. Rev. Lett. **116**, 063005 (2016).
[8] H. L. Bethlem, G. Berden, and G. Meijer, Phys. Rev. Lett. **83**, 1558 (1999).
[9] S. Y. T. van de Meerakker, H. L. Bethlem, and G. Meijer, Nat. Phys. **4**, 595 (2008).
[10] X. Wu, T. Gantner, M. Koller, M. Zeppenfeld, S. Chervenkov, and G. Rempe, Science **358**, 645 (2017).
[11] J. L. Bohn, A. M. Rey, and J. Ye, Science **357**, 1002 (2017).
[12] L. Carr, D. Demille, R. Krems, and J. Ye, New J. Phys. **11**, 055049 (2009).
[13] M. D. Di Rosa, Eur. Phys. J. D **31**, 395 (2004).
[14] B. K. Stuhl, B. C. Sawyer, D. Wang, and J. Ye, Phys. Rev. Lett. **101**, 243002 (2008).
[15] J. F. Barry, D. J. McCarron, E. B. Norrgard, M. H. Steinecker, and D. DeMille, Nature (London) **512**, 286 (2014).
[16] S. Truppe, H. J. Williams, M. Hambach, L. Caldwell, N. J. Fitch, E. A. Hinds, B. E. Sauer, and M. R. Tarbutt, Nat. Phys. **13**, 1173 (2017).
[17] H. J. Williams, L. Caldwell, N. J. Fitch, S. Truppe, J. Rodewald, E. A. Hinds, B. E. Sauer, and M. R. Tarbutt, Phys. Rev. Lett. **120**, 163201 (2018).
[18] L. Anderegg, B. L. Augenbraun, E. Chae, B. Hemmerling, N. R. Hutzler, A. Ravi, A. Collopy, J. Ye, W. Ketterle, and J. M. Doyle, Phys. Rev. Lett. **119**, 103201 (2017).
[19] T. A. Isaev and R. Berger, Phys. Rev. Lett. **116**, 063006 (2016).
[20] I. Kozyryev, L. Baum, K. Matsuda, and J. M. Doyle, Chem. Phys. Chem. **17**, 3641 (2016).
[21] I. Kozyryev, L. Baum, K. Matsuda, B. L. Augenbraun, L. Anderegg, A. P. Sedlack, and J. M. Doyle, Phys. Rev. Lett. **118**, 173201 (2017).
[22] J. Lim, J. R. Almond, M. A. Trigatzis, J. A. Devlin, N. J. Fitch, B. E. Sauer, M. R. Tarbutt, and E. A. Hinds, Phys. Rev. Lett. **120**, 123201 (2018).
[23] T. Roussy, W. Cairncross, D. Gresh, K. Ng, J. Meyers, K. Boyce, Y. Zhou, Y. Shagam, J. Ye, and E. Cornell, Bull. Am. Phys. Soc. **63**, 112 (2018).
[24] C. Panda, D. Ang, D. Demille, J. Doyle, G. Gabrielse, J. Haefner, N. Hutzler, Z. Lasner, C. Meisenhelder, B. O'Leary, A. West, E. West, and X. Wu, Bull. Am. Phys. Soc. **63**, 113 (2018).
[25] E. Altuntaş, J. Ammon, S. B. Cahn, and D. DeMille, Phys. Rev. Lett. **120**, 142501 (2018).
[26] I. Kozyryev and N. R. Hutzler, Phys. Rev. Lett. **119**, 133002 (2017).
[27] T. Isaev, A. Zaitsevskii, and E. Eliav, J. Phys. B **50**, 225101 (2017).
[28] M. L. Wall, K. Maeda, and L. D. Carr, Ann. Phys. (Berlin) **525**, 845 (2013).
[29] M. Wall, K. Maeda, and L. D. Carr, New J. Phys. **17**, 025001 (2015).
[30] M. T. Hummon, M. Yeo, B. K. Stuhl, A. L. Collopy, Y. Xia, and J. Ye, Phys. Rev. Lett. **110**, 143001 (2013).
[31] M. Yeo, M. T. Hummon, A. L. Collopy, B. Yan, B. Hemmerling, E. Chae, J. M. Doyle, and J. Ye, Phys. Rev. Lett. **114**, 223003 (2015).
[32] H. Katori, T. Ido, Y. Isoya, and M. Kuwata-Gonokami, Phys. Rev. Lett. **82**, 1116 (1999).
[33] T. H. Loftus, T. Ido, A. D. Ludlow, M. M. Boyd, and J. Ye, Phys. Rev. Lett. **93**, 073003 (2004).
[34] A. Frisch, K. Aikawa, M. Mark, A. Rietzler, J. Schindler, E. Zupanič, R. Grimm, and F. Ferlaino, Phys. Rev. A **85**, 051401 (2012).
[35] A. L. Collopy, M. T. Hummon, M. Yeo, B. Yan, and J. Ye, New J. Phys. **17**, 055008 (2015).
[36] M. Tarbutt, New J. Phys. **17**, 015007 (2015).
[37] M. R. Tarbutt and T. C. Steimle, Phys. Rev. A **92**, 053401 (2015).
[38] E. B. Norrgard, D. J. McCarron, M. H. Steinecker, M. R. Tarbutt, and D. DeMille, Phys. Rev. Lett. **116**, 063004 (2016).
[39] C. L. Chalek and J. L. Gole, Chem. Phys. **19**, 59 (1977).
[40] A. Bernard and R. Gravina, Astrophys. J. Suppl. Ser. **52**, 443 (1983).
[41] M. Wall, K. Hazzard, and A. M. Rey, *From Atomic To Mesoscale: The Role of Quantum Coherence in Systems of Various Complexities* (World Scientific, Singapore, 2015), pp. 3–37.
[42] B. C. Sawyer, B. K. Stuhl, D. Wang, M. Yeo, and J. Ye, Phys. Rev. Lett. **101**, 203203 (2008).
[43] D. J. McCarron, M. H. Steinecker, Y. Zhu, and D. DeMille, Phys. Rev. Lett. **121**, 013202 (2018).
[44] L. Anderegg, B. L. Augenbraun, Y. Bao, S. Burchesky, L. W. Cheuk, W. Ketterle, and J. M. Doyle, Nat. Phys. **14**, 890 (2018).